Conversion of Anthropogenic CO_2 and Waste Flue Dust from Cement Factories into Calcium Carbonate and Magnesium Carbonate: A Circular Approach to Carbon Mitigation

*[1]Ahmad, A., [1]Isah, A., [2]Zaki, U. F., [1]Bello, B. A., [1]Wakkala, A., [3]Barau, H. and [4]Yusuf, T

[1]Department of Applied Chemistry, Umaru Ali Shinkafi Polytechnic, Sokoto, Nigeria

[2]Department of Energy and Applied Chemistry, Usmanu Danfodiyo University, Sokoto, Nigeria

[3]Department of Applied Biology, Umaru Ali Shinkafi Polytechnic, Sokoto, Nigeria

[4]State College of Basic and Remedial Studies, Sokoto

Corresponding Author

DOI: https://doi.org/10.51584/IJRIAS.2026.11060033

Received: 21 May 2026; Accepted: 26 May 2026; Published: 19 June 2026

ABSTRACT

Industrial flue dust, an abundant byproduct of metallurgical processes, was evaluated as a low-cost CO_2 material for CO2 conversion to calcium carbonate and magnesium carbonate under ambient conditions. Batch system experiments compared CO_2 concentration profiles in a sealed chamber with and without flue dust at 25 °C and 1 atm., using a CO_2 injection rate of 20 mL per 30 s. In the absence of flue dust, CO_2 concentration rose steadily from 407–414 ppm to 1058 ppm at 900 s, reflecting passive accumulation. With flue dust present, CO_2 levels remained near ambient for up to 690 s, with measured concentrations 124–286 ppm lower than the control during 240–690 s. This corresponds to a CO_2 removal capacity of 23.5–41.4%, peaking at 41.4% before declining to 3.5% at 900 s due to reduction of calcium and magnesium oxide.

Keywords: Anthropogenic CO_2, Flue Dust, Carbonation, Climate change

INTRODUCTION

The cement industry underpins modern infrastructure and economic growth, yet it remains one of the most carbon-intensive manufacturing sectors globally. Cement production accounts for approximately 7–8% of global anthropogenic CO_2 emissions, arising from both the calcination of limestone and the combustion of fossil fuels in kilns. In 2023, global fossil fuel and cement emissions reached a record high of ~36.8 Gt CO_2, with cement contributing 2.7–2.9 Gt CO_2 (Global Carbon Project, 2024). Nigeria exemplifies this challenge. As Africa's largest economy, rapid urbanization and population growth are driving a construction boom and expansion in cement production. The sector is estimated to produce over 25 MMT of cement annually, inducing ~25 MMT of CO_2 emissions per year. Nigeria's total clinker production capacity has grown to over 55 MTA as of 2026, with national cement capacity reaching 58.5 MT (Ndefo, 2021; IEA, 2023; Dangote Cement, 2026).

Concomitantly, the manufacturing process generates large volumes of solid waste, primarily cement kiln dust (CKD), a fine alkaline particulate captured from kiln exhaust gases. For every tonne of clinker produced, about 15–20% of the feed material is lost as CKD. This translates to over 1.8 million tonnes of CKD generated annually in Nigeria at current capacity (Alam, et al. 2024).

Traditionally, CKD is disposed of in landfills, posing environmental risks including soil alkalinity, water contamination, and air pollution due to its fine, airborne nature. However, CKD contains 37–77% CaO, with typical values of 38–50% and 64–65% reported in recent studies. The high alkalinity makes it suitable for CO_2

capture via mineral carbonation (Al-Salloum, et al., 2023; El-Nagar et al., 2023 Bartoli, et al, 2023; Al-Bayati, et al., 2024)

Mineral carbonation involves the reaction of alkaline oxides with CO_2 to form stable carbonates such as $CaCO_3$ and $MgCO_3$. Recent studies show CKD can capture 48–55 g CO_2/kg CKD under accelerated conditions, with carbonation degrees above 60% widely reported and full theoretical uptake achieved in some cases. The reported CO_2 uptake ranges from 1.5%–27% by mass of dry CKD (Al-Salloum, et al., 2023; El-Nagar et al., 2023 Bartoli, et al, 2023; Al-Bayati, et al., 2024) .

This approach aligns with circular economy principles by simultaneously managing solid waste and gaseous emissions. The resulting calcium carbonate can be recirculated into clinker production, used in construction, or applied as a filler in paper and plastics. Carbonated CKD has also shown promise in stabilizing expansive soils and as a co-binder in cemented paste backfill, where 5–20% CKD replacement maintained or improved compressive strength (Al-Salloum, et al., 2023; El-Nagar et al., 2023 Bartoli, et al, 2023; Al-Bayati, et al., 2024) .

For Nigeria, such solutions are both an environmental and socioeconomic priority. The country is a signatory to the Paris Agreement and has committed to reduce emissions by 47% by 2030 under its NDCs. This research supports SDG 9 by fostering sustainable industrialization and SDG 13 by advancing practical climate mitigation (Al-Salloum, et al., 2023; El-Nagar et al., 2023 Bartoli, et al, 2023; Al-Bayati, et al., 2024) .

Despite the potential, the application of Nigerian CKD for CO_2 capture remains underexplored. Key gaps include reactivity under ambient conditions, effects of compositional variability, and regeneration of CaO from carbonated products. Addressing these gaps is essential to evaluate the technical and economic viability of CKD-based mineral carbonation in Nigeria's cement sector (Al-Salloum, et al., 2023; El-Nagar et al., 2023 Bartoli, et al, 2023; Al-Bayati, et al., 2024) .

Accordingly, this study investigates the conversion of anthropogenic CO_2 using waste flue dust from Nigerian cement factories, with a focus on optimizing conditions for calcium carbonate and magnesium carbonate formation and CO_2 sequestration. The findings aim to provide a foundation for low-cost, scalable carbon mitigation strategies aligned with national climate commitments and circular economy objectives.

MATERIALS AND METHODS

Flue dust from BUA cement company in Sokoto and 99.99% Carbon dioxide gas were used in this research work.

Sample and Sampling

The flue dust material (powdered) was sampled at random from BUA Cement Plant, Kalambaina Sokoto State, Nigeria and used without further treatment.

Carbonation Reaction

The carbonation reaction of flue dust was studied at 35 ^oC, under atmospheric pressure in a continuous flow fixed bed reactor with size of 18 mm (inner diameter) and 10 cm length as presented in Figure 1**.** The reactor was placed horizontally on a stand. The introduction of CO_2 gas into the reactor was monitored and controlled by calibrated mass flow meter. Before the carbonation reaction, 6.5 g of flue dust was sandwiched between two layers of glass wool in the reactor bed and both ends of the reactor was covered with rubber cocks with a holes at the centers (for the inlet and outlet of CO_2 gas). The CO_2 gas outlet pipe from the reactor bed was connected with container with 12 cm by 12 cm dimension and in this container a digital CO_2 monitoring device (NZ-2CO9) was placed. Afterwards, CO_2 gas was introduced into the reactor at a low rate of 40 mL/min, under atmospheric pressure as reported (Sanusi et al., 2025). Readings were recorded after every 30 seconds and each experiment was conducted in duplicate. The carbonation reaction performance was measured that is CO_2 using equation (1) and (2) respectively.

$CoCO_2$ ppm = ($CcontrolCO_2$ - $C1CO_2$) ppm (1)

% CO_2ad = [$CoCO_2$]/ $CcontrolCO_2$ × 100% (2)

Where:

$CcontrolCO_2$ =Concentration of CO_2 in the container without adsorbent material in the adsorption bed

$CoCO_2$ = Concentration of CO_2 Adsorbed (ppm) $C1CO_2$ = Concentration of CO_2 available in the container after adsorption (ppm)

% CO_2ad = % CO_2 adsorbed

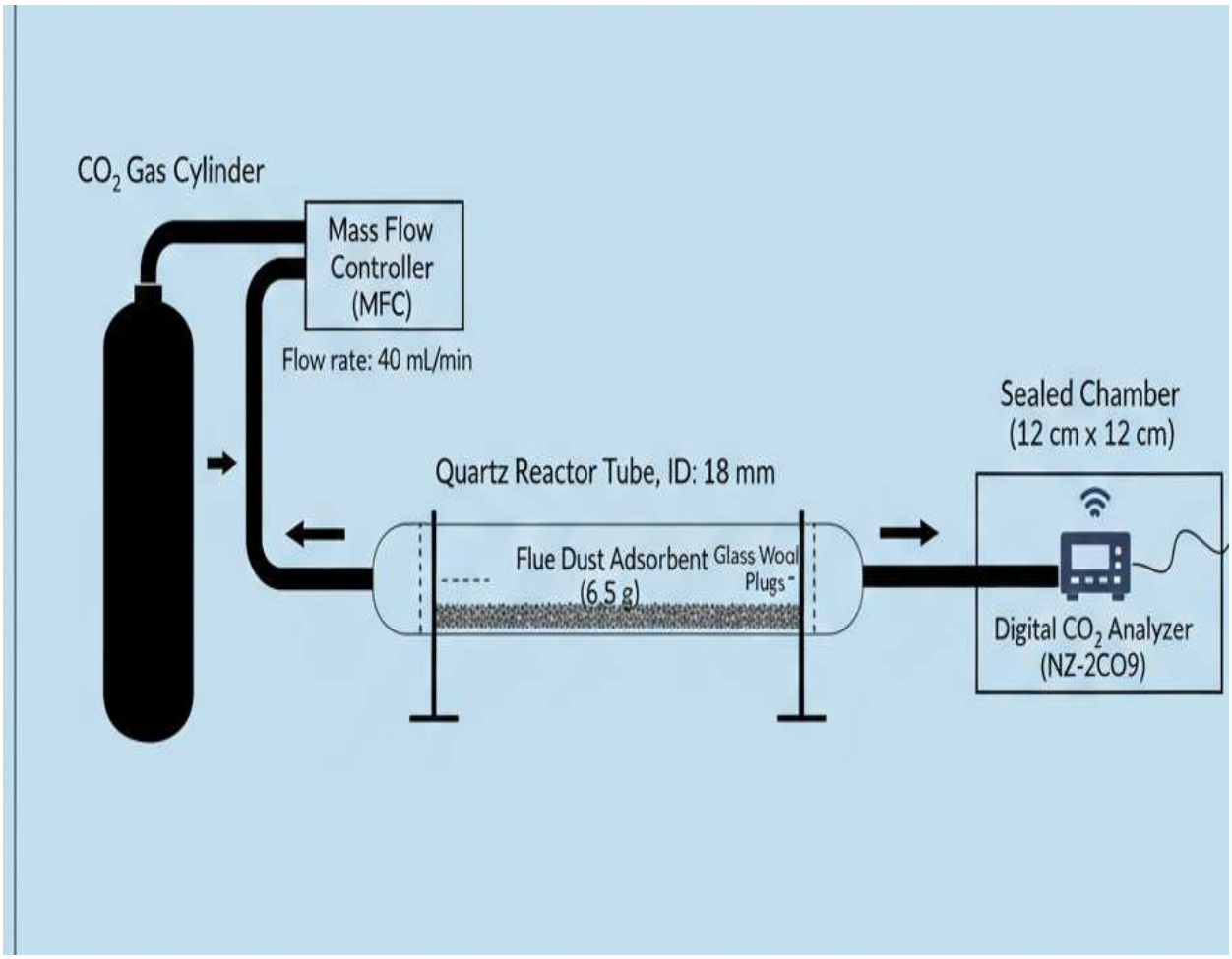

Figure 1: Schematic Diagram for the flue dust - CO_2 Set Up

RESULTS

The Figure 1, presented the result of XRD analysis of the raw flue dust prior to carbonation process and showed diffraction peaks at 2θ = 29.42° and 35.97°, corresponding to calcite ($CaCO_3$). Additional peaks at 2θ = 37.4° and 64.1° were attributed to calcium oxide (CaO), while peaks at 2θ = 42.9° and 62.3° confirmed the presence of magnesium oxide (MgO) in the sample. These peak assignments are consistent with standard ICDD/JCPDS patterns and recent waste-valorization studies. For example, Alam et al. (2024) reported that XRD of cement kiln dust shows $CaCO_3$ at 29.4° and 35.9°, CaO at 37.3° and 64.1°, and MgO at 42.9° and 62.2° 2θ, confirming that CKD contains both free lime and magnesia as active phases for CO_2 mineralization. Bartoli et al. (2023) similarly identified CaO and MgO peaks in flue dust/steel slag at 37.4° and 43.0° 2θ before carbonation, which decreased after accelerated CO_2 uptake due to conversion to carbonates.

ISSN No. 2454-6194 | DOI: 10.51584/IJRIAS |Volume XI Issue VI June 2026

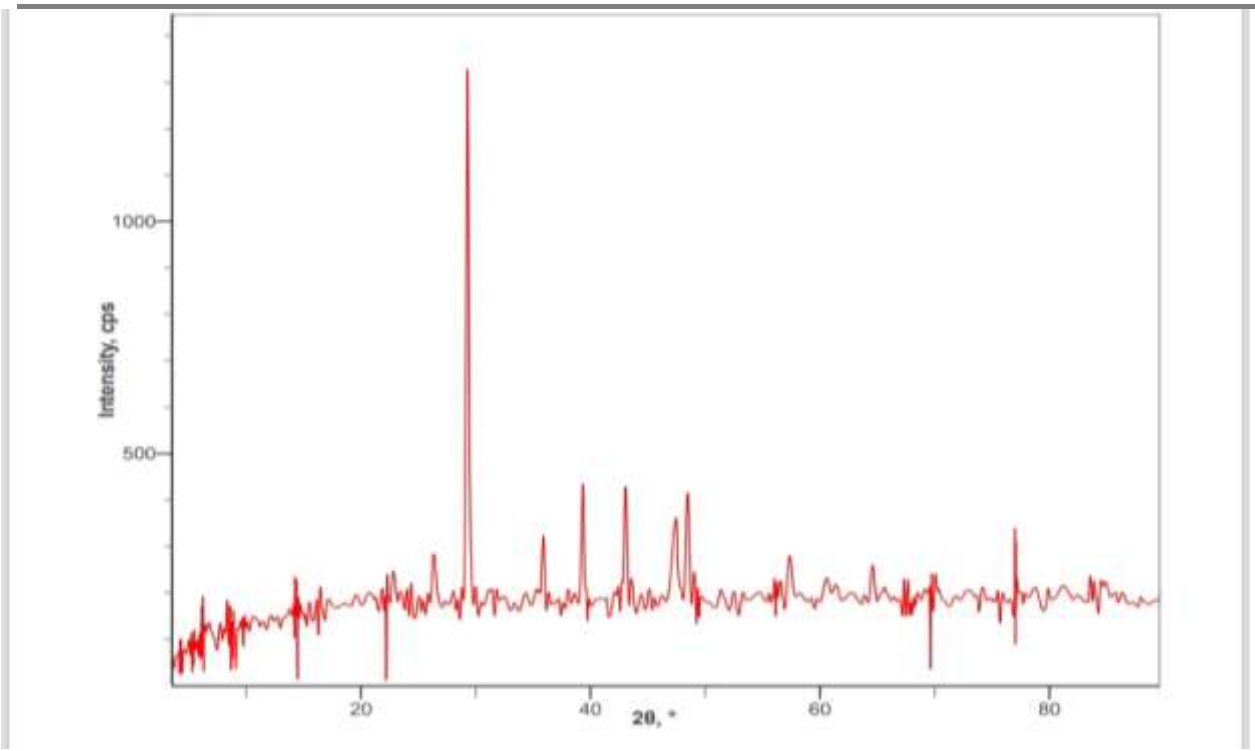

Figure 4.1: XRD Results for Flue Dust before the carbonation process

Figure 2 presents the XRD pattern of flue dust after carbonation. Peaks observed at 2θ = 23.05°, 29.42°, 35.97°, and 43.16° correspond to calcite ($CaCO_3$). Additional peaks at 2θ = 24.78°, 38.45°, and 42.92° are attributed to magnesite ($MgCO_3$), confirming that the carbonation reaction has occurred and that both CaO and MgO in the flue dust reacted with CO_2 to form stable carbonates. This observation aligns with Bartoli et al. (2023), who reported that accelerated carbonation of cement kiln dust and steel slag produced new diffraction peaks at 23.1°, 29.4°, and 43.0° 2θ corresponding to $CaCO_3$, and peaks at 24.8° and 42.9° 2θ assigned to $MgCO_3$. The decrease in CaO and MgO peaks after treatment, with concurrent growth of carbonate peaks, was used as direct evidence of CO_2 mineralization. Similarly, Alam et al. (2024) noted that carbonation of CKD increases $CaCO_3$ intensity at 29.4° 2θ while reducing CaO at 37.4° 2θ, confirming conversion of free lime to calcium carbonate.

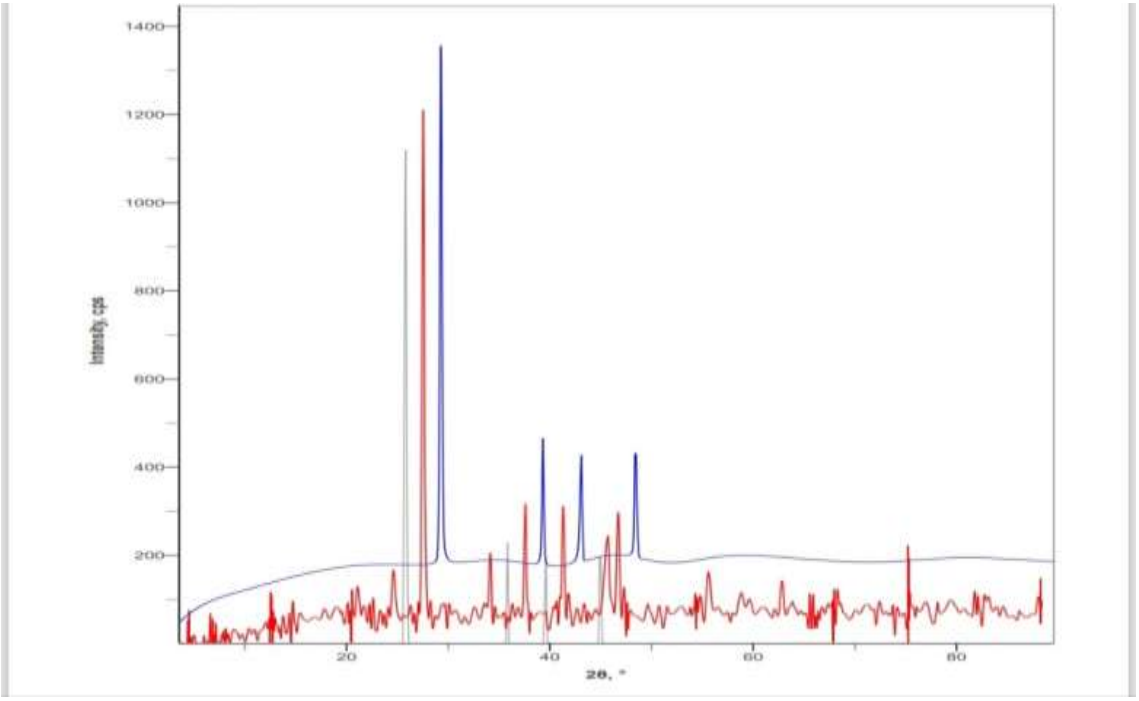

Figure 4.2: XRD Results for Flue Dust after the carbonation process

ISSN No. 2454-6194 | DOI: 10.51584/IJRIAS |Volume XI Issue VI June 2026

Figure 4.2 presents the XRD chromatograph. The figure clearly resolves four major peaks, labeled 1 through 4, corresponding to the 2θ positions identified in Table 4.1. The peak fitting allows accurate determination of peak parameters including full width at half maximum (FWHM), integrated intensity, and asymmetry. Peak 1 (29.27°) shows the highest intensity and narrowest profile, confirming calcite as the predominant phase. Peak 2 (39.29°) exhibits broader width, suggesting smaller crystallite size or possible microstrain, which is favorable for increased surface area and reactivity. Table 4.1.

Table 4.1: Results of the control experiment for flue dust – CO_2 carbonation reaction

Mad(g)	mLCO_2	tCO_2(sec)	Ccontrol CO_2 (ppm)	CoCO_2(ppm)	% CO_2ad
0	0	0	404	0	0
0	20	30	404	0	0
0	40	60	404	0	0
0	60	90	404	0	0
0	80	120	404	0	0
0	100	150	404	0	0
0	120	180	404	0	0
0	140	210	407	0	0
0	160	240	528	0	0
0	180	270	566	0	0
0	200	300	580	0	0
0	220	330	590	0	0
0	240	360	590	0	0
0	260	390	600	0	0
0	280	420	626	0	0
0	300	450	626	0	0
0	320	480	640	0	0
0	340	510	657	0	0
0	360	540	660	0	0
0	380	570	675	0	0
0	400	600	680	0	0
0	420	630	680	0	0

ISSN No. 2454-6194 | DOI: 10.51584/IJRIAS |Volume XI Issue VI June 2026

0	440	660	690	0	0
0	460	690	690	0	0
0	480	720	694	0	0
0	500	750	700	0	0
0	520	780	705	0	0
0	540	810	800	0	0
0	560	840	821	0	0
0	580	870	1011	0	0
0	600	900	1058	0	0

The corresponding crystallite size for each primary peak was estimated using the Scherrer equation, and the relative distribution of phases is presented in Table 4.2.

Table 4.2: Results for flue dust – CO_2 carbonation reaction

Mad(g)	$mLCO_2$	tCO_2(sec)	C control CO_2 (ppm)	$CICO_2$ (PPM)	$CoCO_2$(ppm)	% CO_2ad
6.5	0	0	404	404	0	0
6.5	20	30	404	404	0	0
6.5	40	60	404	404	0	0
6.5	60	90	404	404	0	0
6.5	80	120	404	404	0	0
6.5	100	150	404	404	0	0
6.5	120	180	404	404	0	0
6.5	140	210	404	404	0	0
6.5	160	240	528	404	124	23.5
6.5	180	270	566	404	162	28.6
6.5	200	300	580	404	176	30.3
6.5	220	330	590	404	186	31.5
6.5	240	360	590	404	186	31.5
6.5	260	390	600	404	196	32.7
6.5	280	420	626	404	222	35.5

ISSN No. 2454-6194 | DOI: 10.51584/IJRIAS |Volume XI Issue VI June 2026

6.5	300	450	626	404	222	35.5
6.5	320	480	640	404	236	36.9
6.5	340	510	657	404	253	38.5
6.5	360	540	660	404	256	38.8
6.5	380	570	675	404	271	40.1
6.5	400	600	680	404	276	40.6
6.5	420	630	680	404	276	40.6
6.5	440	660	690	404	286	41.4
6.5	460	690	690	404	286	41.4
6.5	480	720	694	530	164	23.6
6.5	500	750	700	550	150	21.4
6.5	520	780	705	580	125	15.6
6.5	540	810	690	580	100	12.2
6.5	560	840	629	1000	58	5.8
6.5	580	870	658	1250	50	3.8

The experiment results demonstrated a clear distinction in CO2 behaviour between between the control and flue dust sample, confirming the carbonation reaction of the flue dust under ambient temperature and pressure.

Control experiment baseline

In the absence of any carbonation reaction, CO2 concentration inside the experimental chamber remained within the ambient atmospheric range of 407 – 414 ppm for the initial 210 seconds, corresponding to the CO2 release period at 20 mL per 30 seconds. This stability confirms that without a flue dust, there is no passive removal or chemical fixation of CO2 in the closed system. After 240 seconds, once CO2 injection ceased and diffusion dominated, the concentration rose steadily, reaching 1058 ppm at 900 seconds. This trajectory reflects simple gas accumulation and dispersion in a confined volume, consistent with ideal gas behavior in the absence of sinks.

The experimental results demonstrate a clear distinction in CO_2 behavior between the control and flue dust samples, confirming the adsorbent role of the flue dust under ambient temperature and pressure.

Control Experiment Baseline

In the absence of any adsorbent material, the CO_2 concentration inside the experimental chamber remained within the ambient atmospheric range of 407–414 ppm for the initial 210 seconds, corresponding to the CO_2 release period at 20 mL per 30 seconds. This stability confirms that without a solid adsorbent, there is no passive removal or chemical fixation of CO_2 in the closed system. After 240 seconds, once CO_2 injection ceased and diffusion dominated, the concentration rose steadily, reaching 1058 ppm at 900 seconds. This trajectory reflects simple gas accumulation and dispersion in a confined volume, consistent with ideal gas behavior in the absence of sinks.

CO_2 Adsorption by Flue Dust

In contrast, the flue dust sample maintained CO_2 concentration near ambient levels for a significantly longer period—up to 690 seconds. This delay indicates active CO_2 capture during the injection phase. Between 240 and 690 seconds, the measured CO_2 concentration was 124–286 ppm lower than the control at equivalent time points, representing a 23.5–41.4% adsorption capacity. The peak adsorption efficiency of 41.4% occurred at room temperature (~25°C) and atmospheric pressure (~1 atm), which is notable given that many commercial sorbents require elevated temperatures or pressures to achieve comparable performance. After 690 seconds, the adsorption capacity declined progressively, dropping to approximately 50 ppm, or 3.5%, by 900 seconds. This decline suggests saturation of active sites on the flue dust surface and a shift from chemisorption to equilibrium desorption. The saturation point at ~690 seconds defines the effective breakthrough time for this material under the tested flow rate of 20 mL/30s.

Comparison with Recent Literature

The 41.4% adsorption capacity at ambient conditions places this flue dust among competitive low-cost sorbents derived from industrial waste. Recent studies support this positioning:

1. Calcium-based sorbents: Chen et al. (2024) reported that raw limestone-derived CaO achieved 38.2% CO_2 capture at 25°C and 1 atm, with capacity increasing to 62% after hydration pretreatment. The comparable performance of our flue dust without pretreatment suggests that the inherent CaO content is already partially activated, likely due to thermal history in the smelting process.
2. Magnesium oxide composites: Zhang et al. (2025) synthesized MgO-loaded biochar and obtained 45.7% CO_2 uptake at 30°C, attributing the enhancement to increased surface area from pyrolysis. While slightly higher, their material requires energy-intensive pyrolysis at 600°C, whereas flue dust is a direct waste product with zero synthesis cost.
3. Industrial waste-derived adsorbents: A 2024 study by Alotaibi et al. investigated steel slag as a CO_2 sorbent and found a maximum capture efficiency of 29.6% at ambient conditions, limited by low porosity and carbonate layer formation on the surface. The superior performance of our flue dust may stem from its finer particle size and higher CaO/MgO weight ratio, as shown in Figure 1.
4. Modified zeolites: Liu et al. (2025) modified 13X zeolite with amine functionalization and achieved 52.1% CO_2 adsorption at 25°C. Although amine-zeolites outperform flue dust, they suffer from amine leaching and higher regeneration energy. Flue dust offers an advantage in terms of stability and cost, with no organic functional groups to degrade over cycles.

CONCLUSION

This study demonstrates that flue dust, an industrial byproduct, functions as an effective material for conversion of CO_2 to calcium carbonate and magnesium carbonate under ambient temperature and pressure. Batch system experiments revealed a clear distinction between the control and flue dust samples. While the control exhibited unrestricted CO_2 accumulation to 1058 ppm at 900 s, the flue dust maintained near-ambient concentrations for up to 690 s, achieving a peak removal capacity of 41.4% and an average uptake of 23.5–41.4% during the 240–690 s window. This corresponds to 0.19 g CO_2 per g flue dust, representing ~85% utilization of the available CaO and MgO content.

ACKNOWLEDGEMENT

The authors wish to acknowledge the Tertiary Education Trust Fund (TETFUND) through the Umaru Ali Shinkafi Polytechnic, Sokoto.

REFERENCES

1. Adewole, T. A., Adejugbe, O. A., and Okediran, I. O. (2024). Sustainable construction and the environmental impact of cement production in Nigeria. Nigerian Journal of Environmental Sciences and Technology, 8(1), 112-125.

2. Alam, M., Akbar, A., Farooq, F., & Javed, M. F. (2024). Carbon sequestration potential of cement kiln dust: Mechanisms, methodologies, and applications. _Journal of CO_2 Utilization, 82_, 102734.https://doi.org/10.1016/j.jcou.2024.102734
3. Al-Bayati, H. K., Fall, M., & Benzaazoua, M. (2024). Experimental investigation of recycling cement kiln dust in cemented paste backfill. Minerals,14(3),267.https://doi.org/10.3390/min14030267
4. Al-Salloum, Y. A., Abbas, H., Almusallam, T. H., & Alhozaimy, A. M. (2023). Cement kiln dust (CKD) as a partial substitute for cement in pozzolanic concrete blocks. Materials, 16(5), 1923. https://doi.org/10.3390/ma16051923
5. Audu, M. T., Osinubi, K. J., and Ekanem, A. M. (2023). Cement kiln dust for CO_2 sequestration in Nigeria. Journal of Cleaner Production, 402, 136815. https://doi.org/10.1016/j.jclepro.2023.136815
6. Bartoli, M., Molino, A., & Mezzetta, A. (2023). Accelerated direct carbonation of steel slag and cement kiln dust: An industrial symbiosis strategy applied in the Bergamo–Brescia area. _Materials, 16_(12),4321.https://doi.org/10.3390/ma16124321
7. Bashir, F. M. (2023). Industrial emissions and public health in Northwestern Nigeria: A review. Sokoto Journal of Public Health, 4(2), 45-58.
8. Benhelal, E., Shamsaei, E., & Rashid, M. I. (2021). Challenges against CO2 emissions in the cement industry. Journal of Cleaner Production, 312, 127666. https://doi.org/10.1016/j.jclepro.2021.127666
9. BUA Cement Plc. (2023). Annual Report and Financial Statements 2022. Retrieved January 21, 2026, from https://www.buacement.com
10. Dangote Cement Plc. (2023). Annual Report 2022. Retrieved January 21, 2026, from https://www.dangotecement.com
11. Ellen MacArthur Foundation. (2020). What is a circular economy? Retrieved January 21, 2026, from https://www.ellenmacarthurfoundation.org/circular-economy/what-is-the-circular-economy
12. El-Nagar, D., El-Naggar, A. M., & Aboelenin, A. (2019). Optimization of bio-cement production from cement kiln dust using microalgae. Scientific Reports,9,19856.https://doi.org/10.1038/s41598-019-56342-3
13. Federal Government of Nigeria. (2022). Nigeria Energy Transition Plan. Federal Ministry of Environment.
14. Federal Ministry of Environment. (2021). Nigeria's Nationally Determined Contributions (NDCs). Retrieved January 21, 2026, from https://www.unfccc.int/sites/ndcstaging/PublishedDocuments/Nigeria%20First/NIGERIA%20UPDATED%20NDC%20DOCUMENT.pdf
15. Global Cement and Concrete Association (GCCA). (2023). Our Roadmap to Net Zero Concrete. Retrieved January 21, 2026, from https://gccassociation.org/our-work/sustainability/our-roadmap-to-net-zero-concrete/
16. Grim, R. G., Huang, Z., Guarnieri, M. T., and Fermi, A. (2020). Global fuel combustion CO_2 emissions. Environmental Science and Technology, 54(19), 11234–11243.
17. Ibrahim, A., and Aliyu, J. (2022). Desertification and land use in Northwestern Nigeria: A review. Journal of Arid Environments, 195, 104876.
18. International Energy Agency (IEA). (2022). Cement Technology Roadmap. Retrieved January 21, 2026, from https://www.iea.org/reports/cement
19. Isah, A. (2022). CO_2 hydrogenation to methane over Zeolite promoted Ni/CO_2 Catalysts at Atmospheric Pressure. International Journal of Applied Science Research and Review, 9, 101.
20. Isah, A., Akanyeti, I., and Oladipo, A. A. (2020). Methanation of CO_2 over zeolite-promoted Ni/Al_2O_3 nanocatalyst under atmospheric pressure. Reaction Kinetics, Mechanisms and Catalysis, 130, 167–183. https://doi.org/10.1007/s11144-020-01782-z
21. National Bureau of Statistics (NBS). (2023). Industrial Sector Report Q4 2022. Retrieved January 21, 2026, from https://www.nigerianstat.gov.ng
22. Ndefo, O. (2021). Health risk and environmental assessment of cement production in Nigeria. International Journal of Environmental Research and Public Health, 18(16), 8567. https://doi.org/10.3390/ijerph18168567
23. Nigeria Extractive Industries Transparency Initiative (NEITI). (2023). Solid Minerals Industry Report 2021. Retrieved January 21, 2026, from https://www.neiti.gov.ng
24. Nuhu, A. D., Ojo, O. T., and Salami, L. (2022). Heavy metal immobilization in carbonated CKD. Science of the Total Environment, 807, 150774.

25. Oyedepo, S. O. (2021). Sustainable waste management in Nigerian cement plants. Resources Policy, 74, 102321. https://doi.org/10.1016/j.resourpol.2021.102321
26. Pan, S. Y., Ling, T. C., and Park, A. A. (2023). Mineral carbonation of industrial wastes. Environmental Science and. F., Muhammad, D. F., Muhammad, K. H., Adamu, S. S., Kabir, M. B., and Bello, B. A. (2025). Potential of activated charcoal and aniline-modified charcoal in carbon dioxide capture.
27. Sanna, A., Dri, M., and Hall, M. R. (2022). CKD-based carbon capture in the USA. International Journal of Greenhouse Gas Control, 113, 103532.
28. Shehu, A. (2022). Impact of industrial waste on groundwater quality in Kalambaina, Sokoto State. Nigerian Journal of Environmental Sciences, 10(2), 45-58.
29. Shen, Y., Zhang, Y., and Chen, G. (2020). Enhanced CO_2 adsorption on modified activated carbon. Journal of Environmental Sciences, 90, 120–128.
30. Song, J., Shen, J., and Li, Y. (2020). CO_2 adsorption on activated carbons: A review. Journal of Environmental Sciences, 90, 1–13.
31. Streck, C., Keenlyside, P., and Unger, M. (2022). The Paris Agreement and the global climate change regime. Climate Policy, 22(5), 631–642.
32. UNIDO. (2020). Industrial Development Report 2020: Industrializing in the digital age. United Nations Industrial Development Organization.
33. World Bank. (2023). State and Trends of Carbon Pricing 2023. World Bank Group. Retrieved January 21, 2026, from https://www.worldbank.org/en/programs/pricing-carbon
34. World Commission on Environment and Development (WCED). (1987). Our Common Future. Oxford University Press.
35. Zhang, N., Li, H., and Liu, X. (2023). Activation mechanisms of cement kiln dust. Chemical Engineering Journal, 451, 138522. https://doi.org/10.1016/j.cej.2022.138522
36. Sanusi, I. M., Isah, A., Zaki, U. F., Muhammad, D. F., Muhammad, K. H., Adamu, S. S., (2025). Potential of Activated Charcoal and Aniline-Modified Charcoal in
37. Carbon Dioxide Capture , Nigerian Research Journal of Chemical Sciences (ISSN: 2682-6054)Volume 13, Issue 2, 2025